Testing, Modeling, and Control of a Fuel Cell Hybrid Vehicle

Min Joong Kim[1], Huei Peng[2], Chan-Chiao Lin[1], Euthie Stamos[3], Doanh Tran[3]

***Abstract*—A comprehensive procedure for testing, modeling, and control design of a fuel cell hybrid vehicle (FCHV) is presented in this paper. The subsystems are modeled based on lab testing and in-field vehicle testing results from the DaimlerChrysler *Natrium* prototype vehicle. An FC-VESIM (fuel cell hybrid vehicle simulation) model is then developed based on the experimental data. The power management control algorithm for the FCHV is subsequently developed based on the stochastic dynamic programming (SDP) technique, which produces an optimal policy for a given probability distribution of the vehicle power demand.**

I. Introduction

Over the last decade, interest in alternative automotive powertrains increases steadily, including hybrid electric vehicles (HEVs) and fuel cell vehicles (FCVs). Proton exchange membrane fuel cells using hydrogen produced from renewable energy sources are widely perceived as an important long-term technology for sustainable personal mobility. The main purpose of this paper is to describe the development of a FCV computer model based on the DaimlerChrysler Town and Country *Natrium* shown in Fig. 1. This model provides the basis for future math-based design, analysis and control design of fuel cell vehicles.

Many major vehicle manufacturers have developed prototype fuel cell vehicles for technology evaluation and demonstration purposes [1, 2, 3]. These vehicles have been used for proof-of-concept, promoting interest of future development and have contributed positively to the public perception and strategy planning of sustainable vehicle technologies. However, since these vehicles are not meant for production, they are put together swiftly. Model-based, systematic development processes that are commonly adopted for traditional (internal combustion engine powered) vehicles, are rarely explored to their full potential in the development of these prototype vehicles.

Academic research groups are also working actively on this emerging technology. Guezennec et al. [4] solved the supervisory control problem of a FCHV as a quasi-static optimization problem and found that hybridization can significantly improve the fuel economy of FCVs. Rodatz et al. [5] used a set of rules for their energy management algorithm, which include high-level goals, such as driver power demand and fuel economy, and component reliability goals, such as hydrogen purging, supercapacitor SOC levels and current limits. The National Renewable Energy Laboratory included a fuel cell system option in its simulation model ADVISOR [6], which can simulate FCVs and HEVs with ease.

Up to today, few papers have published detailed models of a fuel cell vehicle, and exercise state-of-the-art control design approach on a validated fuel cell vehicle model. The main contribution of this paper is to report the modeling and control results from an industry-academic collaboration. The authors combine their strengths on this research. This paper can be viewed as an early "lessons learned" report on the development of this critical future vehicle technology.

Fig. 1. "*Natrium*": DaimlerChrysler fuel cell hybrid vehicle

II. Experimental Setup

A. DaimlerChrysler Town and Country Natrium Vehicle

The vehicle studied in this paper is the DaimlerChrysler *Natrium* prototype vehicle. The powertrain configuration of the *Natrium* is shown in Fig. 2. Major components include a Fuel Cell Engine, a Lithium-Ion Battery, a DC-DC Converter, an Electric Drive, a Hydrogen supplying system, and the vehicle body.

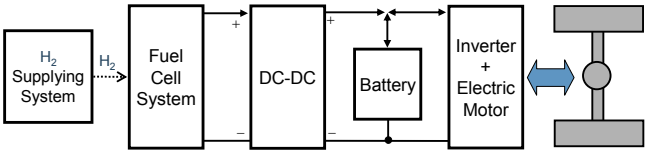

Fig. 2. Schematic configuration of the fuel cell hybrid vehicle "*Natrium*"

The powertrain of *Natrium* consists of an 82 kW peak electric drive system, a 40 kW Li-ion battery pack and a 75 kW fuel cell engine. The vehicle achieved a maximum travel

[1] GSRA, Department of Mechanical Engineering, University of Michigan, Ann Arbor, MI 48109.
[2] Associate Professor, Department of Mechanical Engineering, University of Michigan, Ann Arbor, MI 48109 (734-936-0352, hpeng@umich.edu)
[3] DaimlerChrysler Cooperation

range of about 500 km between fill-ups, a top speed of 133 kph, acceleration from 0 to 100 kph at 16 seconds. The vehicle was tested in various conditions to verify its performances in highway driving, city driving, rapid acceleration, and maximum travel range while experimental data are collected from the vehicle components.

B. Test Bench

Many components of the *Natrium* powertrain were designed specifically for the vehicle. They were bench-tested for factory acceptance before vehicle integration. A test bench was constructed, which enables more precise and controlled testing of individual components. In addition to subsystem function verifications, special-purpose tests were also designed to obtain the necessary data to build dynamic models and efficiency maps of the sub-systems.

The component configuration of the test bench is roughly the same as the Natrium vehicle while an electric power processing system (ABC-150 by AeroVironment) was used to simulate the electric load from the electric drive/vehicle. It is a bi-directional power processing system capable of converting high voltage AC electrical power of the utility consumer power grid to and from high voltage DC.

The DC-DC converter and Lithium-Ion Battery pack were tested using the test bench. Their electrical as well as thermal behaviours were observed with key data recorded.

C. System Interfacing

The component interfacing used is a Controller Area Network (CAN) and a data acquisition tool. For the case of the Natrium vehicle, about 200 channels of data were collected, at the rate of 50 Hz or higher.

III. MODELING

Utilizing the facilities described in section II, subsystems of a FCHV are modeled. For each subsystem, we developed a simple model for fast supervisory-level control design and a more sophisticated model for accurate simulation. In this paper, the focus will be on simple subsystem models for the control design purposes.

A. Fuel Cell System

The fuel cell stack used in our test vehicle is a medium-pressure system. Compressor rotational speed and supply manifold pressure have time constants in the order of a few hundred milliseconds, which are significantly faster than the vehicle longitudinal dynamics. Therefore, if the purpose of the model is for supervisory-level control design, it is appropriate to ignore these state variables. However, for fuel cell breathing control at the servo-level, it would not be possible to ignore those dynamics. Another fuel cell stack dynamic variable is the stack temperature (which may have to be considered together with the stack membrane relative humidity in a highly accurate model). Again for the high-level power management control design purpose, the stack temperature is assumed to be a model parameter in the simulations and analyses. As a first step, we assume that the stack temperature is well regulated by a cooling system, and thus we will focus on the modeling and control design under this given temperature.

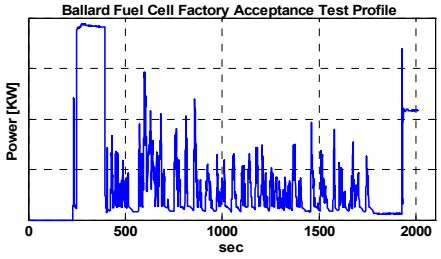

Fig. 3. Factory acceptance test for the fuel cell system

The fuel cell stack voltage is known to be a function of the fuel cell current, stack temperature, reactant partial pressure, and membrane humidity [8]. Due to the fact the fuel cell engine operates at a relatively low pressure (1~2 barg), as well as the fact the fuel cell exhibit a behavior that is closed-loop regulated, the stack voltage was not found to vary significantly with the cathode (air) or anode (hydrogen) pressure. Since stack or membrane humidity information was not known accurately, the following approximation is used:

$$V_{cell} = f(I, T_{stack}, P_{H_2}, P_{air}, \lambda_m ...) \approx f_2(I, T_{stack}) \,. \quad (1)$$

The equation for the cell voltage can be denoted as

$$V_{cell} = E_0 - R\,i - b\ln(i) - m\exp(n\,i) \,. \quad (2)$$

And for curve fitting purpose, Eq.(2) is modified as

$$V_{cell} = c_1 + c_2 \cdot e^{-c_3 \cdot I} - c_4 \cdot I \,. \quad (3)$$

which is used for the polarization curve fitting. From the data collected during the factory acceptance tests, a general polarization curve, as seen in Fig. 3 and a least square curve fitting of two different temperature regions, as seen in Fig. 4, were generated. The voltage variations of the test data are mainly due to transient operations, uncertainty in reactant partial pressure, and humidity.

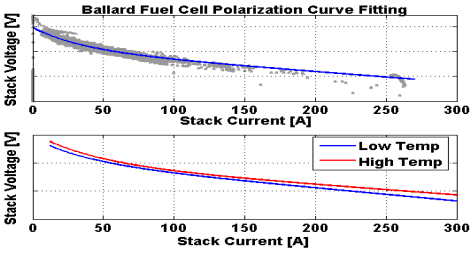

Fig. 4. Polarization curves and temperature effects

The polarization curve only characterizes the stack behavior, and does not truly reflect the system (net) behavior. Once the current drawn by auxiliary loads (such as compressors and fans) in the fuel cell system is obtained, the stack (net) efficiency can be calculated. Fig. 5 shows the relation between the system auxiliary load and the net current. The system efficiency curve as a function of the fuel cell net power is shown as well. The fuel cell system demonstrates satisfactory efficiency at the medium to

high-power regions. There is a slight reduction in system efficiency as the net fuel cell power increases due to the Ohmic loss.

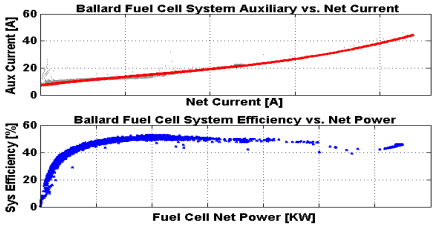

Fig. 5. Fuel cell auxiliary current and system efficiency

B. *Lithium-Ion Battery*

It is very difficult to develop an accurate phenomena-based battery model that can be used to predict transient behaviors because of the complexity of chemical reactions. Most models existing in the literature, suitable for vehicle performance prediction are lumped curve-fitting models. Static battery models such as the Shepherd equation [9] do not explicitly include battery state of charge (SOC) concept. Therefore, we use equivalent RC circuit models and the resistance model (Fig. 6), both described in details in the documentation of the ADVISOR program [6]. The RC circuit model captures the dynamic behaviors of the Li-Ion battery more accurately, whereas the resistance model is easier to build and is adequate for the control algorithm development. We chose to use the RC circuit model which has a state space model show in Eq.(4).

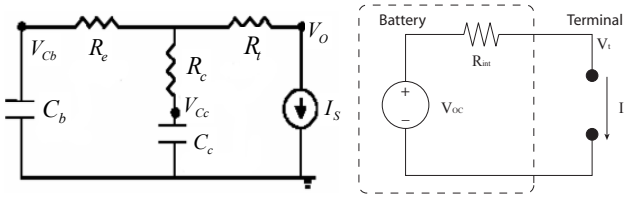

Fig. 6. Battery RC circuit model (left) and one resistant model (right)

$$\begin{bmatrix}\dot{V}_{Cb}\\ \dot{V}_{Cc}\end{bmatrix}=\begin{bmatrix}\frac{-1}{C_b(R_e+R_c)} & \frac{1}{C_b(R_e+R_c)}\\ \frac{1}{C_c(R_e+R_c)} & \frac{-1}{C_c(R_e+R_c)}\end{bmatrix}\begin{bmatrix}V_{Cb}\\ V_{Cc}\end{bmatrix}+\begin{bmatrix}\frac{-R_c}{C_b(R_e+R_c)}\\ \frac{-R_e}{C_b(R_e+R_c)}\end{bmatrix}[I_S] \quad (4)$$

$$[V_O]=\begin{bmatrix}\frac{R_c}{R_e+R_c} & \frac{R_e}{R_e+R_c}\end{bmatrix}\begin{bmatrix}V_{Cb}\\ V_{Cc}\end{bmatrix}+\left[-\frac{R_cR_e}{R_e+R_c}-R_t\right][I_S]$$

The Li-Ion battery pack was tested at selected levels of SOC, between 10% and 100% to get the model parameters. Based on the Hybrid Pulse Power Characterization (HPPC) test suggested in the FreedomCAR battery test manual [10], three consecutive discharging and charging current pulses with 10-second duration and 40 seconds of idling in between, were applied for every selected SOC level (See Fig. 8).

The parameters of the RC circuit battery model are then obtained as optimal data fitting results as functions of SOC (See Fig. 9). In theory, we could also repeat the tests at different temperature. However, this type of testing requires a Climate Control Chamber and we were not able to obtain access. Therefore the battery parameter values are obtained only at room temperature (25°C). The battery internal resistance values as functions of SOC were obtained based on the definitions from the FreedomCAR battery test manual. The results are shown in Fig. 10.

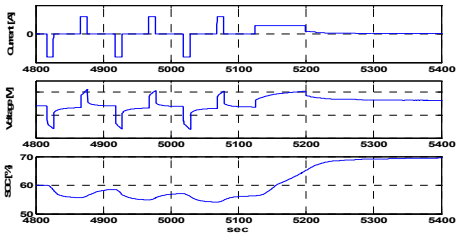

Fig. 8. Current, voltage, SOC signals of battery test

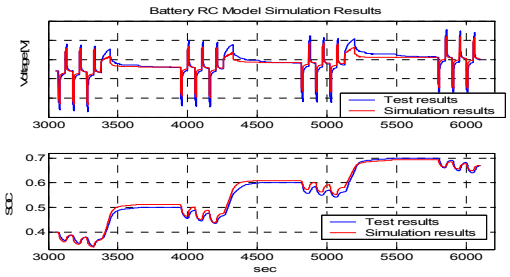

Fig. 9. Battery RC model parameter estimation results

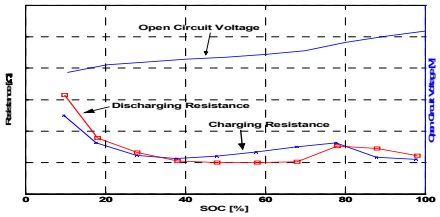

Fig. 10. Battery one resistance parameter estimation results

C. *DC-DC Converter*

Base on the testing results, the DC-DC converter is described as a second order dynamic system in our simulation model. Its response rate is slowed down deliberately to protect the fuel cell. Nevertheless, its response is still fast enough compared to that of the vehicle longitudinal dynamics. For the simple model, the DC-DC converter is described as a static device with efficiency loss, which is a function of the fuel cell output power. The power demand under the US06 cycle is used to study the input/output behavior of the DC-DC converter. The fuel cell side (input side) power and the conversion efficiency are shown in Fig. 11. The converter efficiency is higher than 95% in most of the operating range. An exponential curve, as shown in (5), was found to fit the efficiency data well (See Fig. 12).

$$\eta_{DC/DC}=\alpha_1+\alpha_2\cdot\exp\left(-\alpha_3\cdot P_{fuelcell}\right) \quad (5)$$

where $\alpha_1, \alpha_2, \alpha_3$: constants, $P_{fuelcell}$: fuel cell side power [kW]

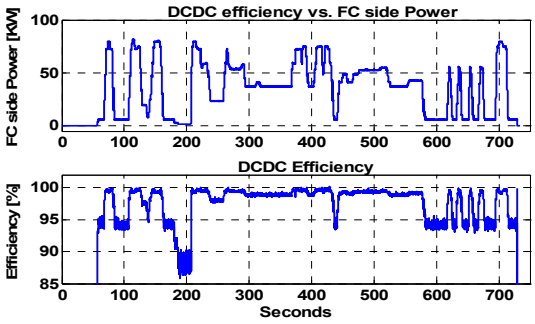

Fig. 11. DC-DC converter test profile and corresponding efficiency

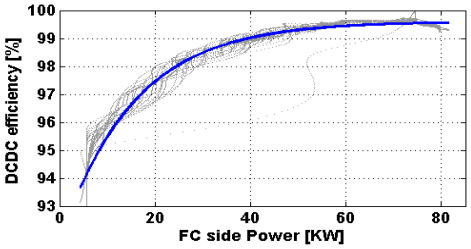

Fig. 12. DC-DC converter efficiency versus fuel cell side power

D. Electric-Drive

The *Natrium* is equipped with an 82 kW (peak) 3 phase AC motor. For this drive system, a steady-state model (Fig. 13) was used. Given the torque, motor speed, and the electric bus voltage, this 3D look-up table gives the required electric power as an output. This accurate motor map captures the effect of the bus voltage on motor efficiency whereas other simple motor efficiency maps do not.

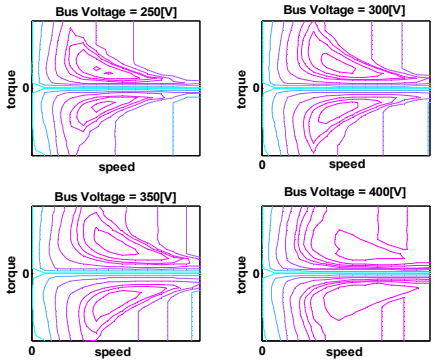

Fig. 13. Electric drive efficiency 3-D look-up table

The efficiency of the electric-drive is defined as the ratio between the supplied power the converted power. Obviously, due to the fact the electric drive can operate as either a motor or a generator, the definition of input/output sides is reversed when the electric drive is operated in the regenerative mode. Considering both operation modes, the efficiency of the electric drive is defined as

$$\eta_{mot} = \left| \frac{\tau_{mot} \cdot \omega_{mot}}{V_{DC} \cdot I_{DC}} \right|^{k}, \text{where } k = \pm 1 \text{ (discharging/charging)} \quad (6)$$

Equation (6) can be significantly affected by phase lag between signals due to the motor inertia. Therefore we selected specific data satisfying quasi-steady state conditions and calculated corresponding efficiency for the validation purpose. The calculated two-dimensional efficiency map was found to be qualitatively close to the look-up tables.

IV. VALIDATION OF THE FC-VESIM MODEL

A FC-VESIM (**f**uel **c**ell hybrid **ve**hicle **sim**ulation) model was constructed based on the VESIM model developed at the University of Michigan. This model consists of several subsystems: driver, fuel cell, battery, power bus (including DC-DC converter), electric-drive and vehicle. The subsystems were from the empirically verified models described in Section III and the parameters of the vehicle block were based on the *Natrium*, for which the speed is calculated from a point-mass longitudinal vehicle dynamics.

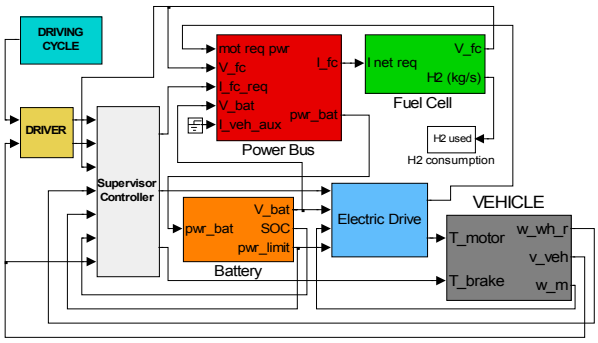

Fig. 15. The FC-VESIM model

Even though each subsystem is modeled and validated separately, the FC-VESIM simulation model needs to be checked to confirm that the overall model works properly. The validation was done by comparing predicted results with test results obtained under a "near-wide-open-throttle" vehicle launch (Fig. 16). For the purpose of the virtual vehicle validation, the fuel cell current request command and motor power request signal were given to the simulation model. Selected sub-system response signals are presented in Figures 17-20. It can be seen that most of the model predictions are very close to the test results. Battery response is perhaps the only one that shows very noticeable difference, possibly due to the variation in environmental temperature and battery aging. The validation results confirm that the FC-VESIM model is reasonably accurate and seems to be suitable for math-based vehicle development.

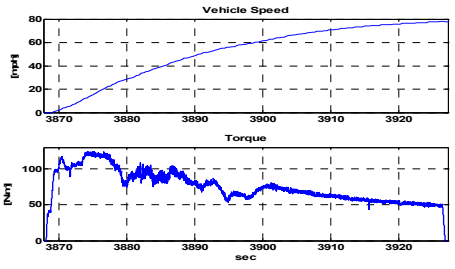

Fig. 16. *Natrium* vehicle road test profile for the FC-VESIM validation

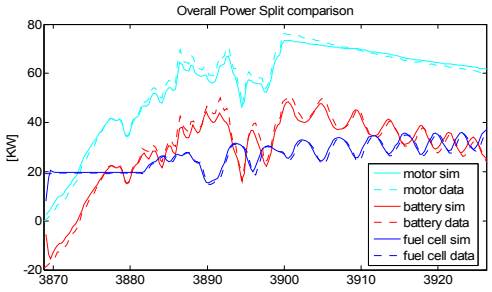

Fig. 17. Power split comparison between simulation results and test data

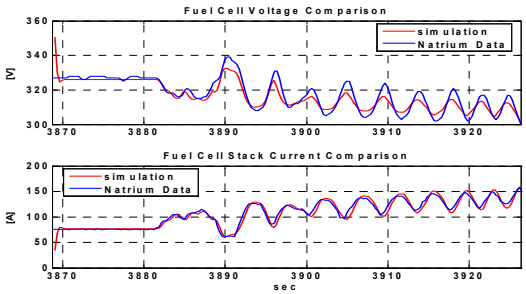

Fig. 18. Fuel cell component validation

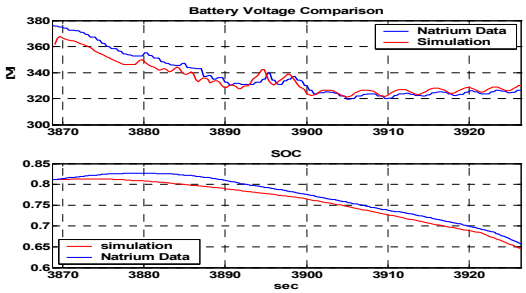

Fig. 19. Battery component validation

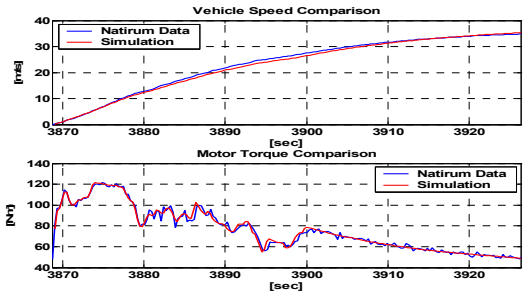

Fig. 20. Vehicle component validation

V. CONTROL STRATEGY DEVELOPMENT

With a high-fidelity model available, we decided to use a model-based design approach to explore the full potential of this fuel cell powertrain. We first simplified the FC-VESIM model to contain only 2 states (wheel speed and battery SOC), which is subsequently converted into a discrete format. The power management controller is designed by using the stochastic dynamic programming (SDP) technique [11] to ensure optimal fuel economy. The key idea of the SDP approach is that the driver power demand is modeled as a Markov chain model, i.e., the power demand from the drive at the next time step depends on the current power demand and vehicle speed:

$$p_{il,j} = \Pr\left\{ w = P_{dem}^{j} \middle| P_{dem} = P_{dem}^{i}, \omega_{wh} = \omega_{wh}^{l} \right\} \quad \text{for } i, j = 1,2,...,N_p, \quad l = 1,2,...,N_\omega \tag{8}$$

where the power demand P_{dem} and the wheel speed ω_{wh} are quantized into grids of N_p and N_ω respectively. To construct the transition probability function, four different driving cycles including city, suburban, and highway driving scenarios are selected. From these cycles, the corresponding P_{dem} and ω_{wh} at each time step was calculated by the inverse vehicle model. The sequence of observations (P_{dem}, ω_{wh}) was mapped to a sequence of quantized states $(P_{dem}^{i}, \omega_{wh}^{l})$. Then we got the transition probability p by counting all transitions.

The objective of the SDP optimization problem is to find an optimal control policy $u = \pi(x)$, which maps observed states (i.e., SOC, wheel speed, and power demand) to control decision (i.e., fuel cell current request) while minimizes the expected cost of hydrogen consumption and battery energy usage over an infinite horizon:

$$J = \lim_{N\to\infty} \underset{w_k}{E}\left\{ \sum_{k=0}^{N-1} \gamma^k \left(W_{H_2,rct} + \alpha M_{soc} \right) \right\} \tag{9}$$

where $0 < \gamma < 1$: discount factor, α: weighting factor

$W_{H_2,rct}$: H_2 consumption, $M_{soc} = \left(SOC - SOC_{ref}\right)^2$

Based on Bellman's optimality equation, the SDP problem can be solved by a policy iteration, which conducts a policy evaluation step and a policy improvement step in an iterative manner until the optimal cost function converges [12]. The approximate value function for a given policy, $J_\pi(x)$, is first calculated by iteratively updating the Bellman equation in the policy evaluation step:

$$J_\pi^{s+1}(x^i) = g(x^i, \pi(x^i)) + \underset{w}{E}\left\{ \gamma J_\pi^{s}(x') \right\} \tag{10}$$

for all state grid i, where s is the iteration number, and x' is the new states evolving from x^i based on dynamic equations. Subsequently, an improved control policy can be obtained from the updated approximate value function in the policy improvement step:

$$\pi'(x^i) = \underset{u\in U(x^i)}{\operatorname{argmin}} \left[g(x^i, u) + \underset{w}{E}\left\{ \gamma J_\pi(x') \right\} \right] \tag{11}$$

for all i, where J_π is the approximate cost function obtained from the policy evaluation step. After the new policy is obtained, we go back to the policy evaluation step to update the cost function using the new policy. This iterative process is repeated until J_π converges within a selected tolerance level.

The obtained control policy $I_{fc,req} = \pi^*(SOC, \omega_{wh}, P_{dem})$ is a full-state feedback algorithm and calculates the fuel cell current demand to the DC-DC converter based on the three state variables. Fig. 21 shows two cross sections of the 3-D

map. One distinctive feature of the controller is that it considers vehicle speed in the control policy whereas many other heuristic hybrid controllers do not.

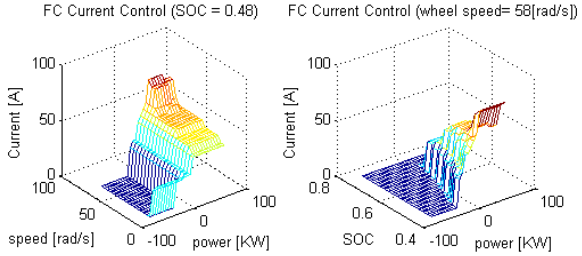

Fig. 21. Two cross sections of the 3-D-map SDP controller

Example time-trace of the power distribution simulation results are shown in Fig. 22. It can be seen that the fuel cell provides the bulk of the power while the battery helps with the transient. Fig. 23 shows that the SDP controller runs the fuel cell system largely around the most efficient operating region. The miles per gallon gasoline equivalent (mpgge) based on the hydrogen lower heating value of Natrium simulation is roughly twice that of a gasoline-powered Town and Country® minivan, upon which Natrium is based.

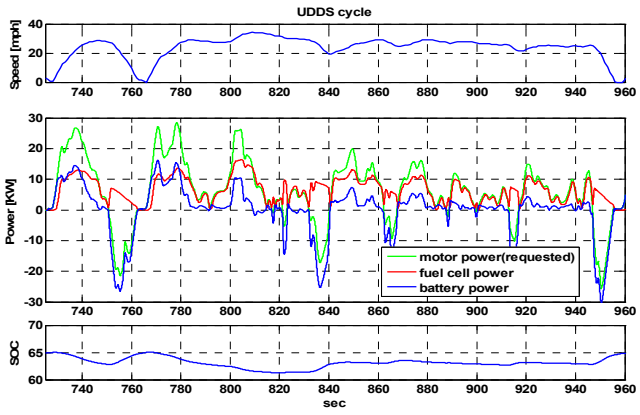

Fig. 22. Power split and SOC simulation using the SDP controller (part of the UDDS cycle)

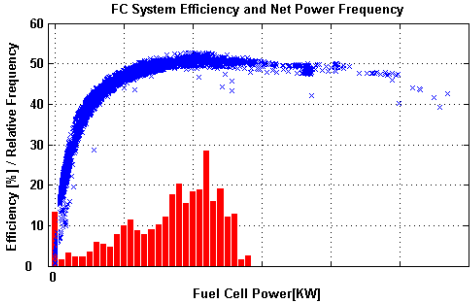

Fig. 23. Fuel cell system efficiency and net power frequency histogram

TABLE I. FUEL ECONOMY COMPARISON

	Cycle	mpg (mpgge*)
NATRIUM Simulation Using the SDP Controller	Highway	43.4*
	City	41.7*
DaimlerChrysler Town and Country® (gasoline engine)	Highway	25.0
	City	18.0

* mpgge : 1kg $H_2 \approx$ 1gallon Gasoline (based on the lower heating value of hydrogen)

VI. CONCLUSIONS

A dynamic fuel cell vehicle model was developed through collaboration between DaimlerChrysler and the University of Michigan. The model is developed based on test results obtained on the *Natrium* prototype vehicle and a test rig. The subsystems are first modeled by examining input/output data from carefully designed tests. A vehicle model is then constructed by following the configuration used in the *Natrium.* Model validation results confirm that the forward-looking simulation model predicts vehicle performance accurately. The stochastic dynamic programming methodology was introduced to obtain a power management algorithm to optimize vehicle fuel economy while ensuring drivability. The fuel cell vehicle achieves a fuel economy favorably compared against its gasoline counterpart. These preliminary results lay a good foundation for future model-based fuel cell vehicle development process, currently being developed by DaimlerChrysler and the University of Michigan.

REFERENCES

[1] T. Ishikawa, et al., "Development of Next Generation Fuel-Cell Hybrid System—Consideration of High Voltage System," *SAE Paper*, No.2004-01-1304

[2] A. Ohkawa, "Electric Power Control System for a Fuel Cell Vehicle Employing Electric Double-Layer Capacitor," *SAE Paper*, No. 2004-01-1006

[3] C.-G. Cantemir, C. Hubert, G. Rizzoni, B. Demetrescu, "High Performance Fuel Cell Sedan," *SAE Paper*, No. 2004-01-1003

[4] Y. Guezennec, T.-Y. Choi, G. Paganelli, G. Rizzoni , "Supervisory Control of Fuel Cell Vehicles and its Link to Overall System Efficiency and Low-Level Control Requirements," *Proceedings of the American Control Conference*, Denver, CO. 2003

[5] P. Rodatz, et al., "Performance and Operational Characteristics of a Hybrid Vehicle Powered by Fuel Cells and Supercapacitors," *SAE paper*, No. 2003-01-0418

[6] T. Markel, *et al*., "ADVISOR: a systems analysis tool for advanced vehicle modeling," *Journal of Power Sources,* Vol. 110, 2002, pp. 255-266

[7] M.J. Ogburn, et al., "Modeling and Validation of a Fuel Cell Hybrid Vehicle," *SAE paper*, No. 2000-01-1566

[8] J. Pukrushpan, A.G. Stefanopoulou, H. Peng, *Control of Fuel Cell Power Systems: Principles, Modeling, Analysis and Feedback Design*. Springer, London, 2004

[9] C.M. Shepherd, "Design of Primary and Secondary Cells—II, An Equation Describing Battery Discharge," *Journal of the Electrochemical Society*, Vol.112, No.7, 1965, pp.657-664.

[10] USDOE, *FreedomCAR Battery Test Manual for Power-Assist Hybrid Electric Vehicles, DOE/ID-11069, Contract DE-AC07-99 ID13727*, October, 2003

[11] C.C. Lin, H. Peng, J.W. Grizzle, "A Stochastic Control Strategy for Hybrid Electric Vehicles," *Proceedings of the American Control Conference*, Boston, MA, 2004

[12] M.L. Puterman, *Markov Decision Processes: Discrete Stochastic Dynamic Programming*. J. Wiley, New York, NY., 1994